11 May 2012

GEM Magnetosheath FG white paper

Modeling and Data-analysis of the 'Steady-state' Magnetosheath

Contents

1. Motivation

The goal of this white paper is to bring together in a single document all of the issues and considerations relevant to comparisons between spacecraft observations, numerical models, and analytic models for the purpose of developing a more complete description of the 'steady state' magnetosheath. It is intended that, as this goal is pursued, methodologies and metrics will be established by which more meaningful (i.e., quantitative) comparisons can be made. This is to be a 'living' document, in that it may be edited by interested parties as new methodologies, metrics, and models are developed. However, the master copy will be held by the Geospace Environment Modeling Magnetosheath Focus Group leaders; Steve Petrinec and Katariina Nykyri.

A secondary goal is to create an on-line library (with mirror sites). This library will house copies of magnetosheath observation data sets (along with associated solar wind data sets), and various analyses of the data; especially of synoptic maps of the magnetosheath region of the various physical parameters for different solar wind conditions. Each such analysis and map will be accompanied with a header file that explicitly describes which assumptions were used in its creation (this will be described in greater detail in the Appendix). Similar header files will also be included for all numerical model runs which are included in the library. Lastly, analytic models as simple-to-run code modules and detailed README files (with relevant information in the same header format) will also be included in this library. The intent is that such a library with detailed descriptions of all assumptions used will make it easier to produce meaningful, quantitative comparisons between different models.

2. Introduction

An underlying assumption of this endeavor is that the magnetosheath region is reasonably constant in shape and size when the solar wind is steady. It is generally recognized that this is not truly the case. For example, shock reformation processes occur (well-known at the quasi-parallel shock region), for which there are large-amplitude waves steepen upstream and downstream of an ill-defined 'shock front'. In addition, a long period of steady, southward IMF will continue to erode the dayside magnetopause (as does a steady northward IMF reduces the width of the magnetotail). Thus, it is necessary to state up front that the models produced from observations, numerical runs, and analytic models are merely zeroth-order, idealized representations of the steady-state magnetosheath (and may be thought of as a 'snap-shot' in time), upon which dynamic processes (even while the solar wind is steady) can be treated as higher order perturbations to the magnetosheath shape, size, and properties.

It is often touted that observations have the final say as to the properties of the magnetosheath region. While true, it is to be noted that as important as the observations in and of themselves are, it is at least as important that they are treated and parameterized properly. There are always many assumptions to be applied to the data sets; some of which are weak and trivial, and others for which the conclusions drawn are strongly dependent.

Numerical models have different sets of issues and concerns; from the high-level concerns as to, e.g., whether MHD captures enough of the relevant physics to the more detailed concerns of mass ratios and numerical instabilities.

Current analytic/theoretical models, while often elegant and usually easy to use, provide an ideal representation of the magnetosheath that may reflect some of the major aspects of the real magnetosheath; but often misses much. Nevertheless, these models are necessary tools for studying large scale behavior.

The reader is reminded that the hydrodynamic numerical model runs with embedded magnetic field and resulting contour plots produced by Spreiter *et al*. in 1966 are still often used as a basis for comparison in a significant percentage of analyses done today. If the community is to move beyond this early attempt to model the magnetosheath region, then there needs to be a definitive push to develop magnetosheath 'steady state' models which are easy-to-use and with all assumptions explicitly described.

The remainder of this white paper is ordered as follows: First, commonly known issues and assumptions regarding the treatment of the magnetosheath region based on observations are examined in detail. Next, the same procedure is applied to the current numerical models. Lastly, the current analytic models are discussed. The Magnetosheath Focus Group Challenge is next included. The Appendix describes a table (header file) which is intended to be filled out and included with each analysis, model, and simulation run that enters the magnetosheath on-line library. While individual data sets and model strengths and weaknesses are described in detail in this document, there is no intention to either champion, demean, or belittle the hard work of all that has gone into these efforts. Rather, it is only intended that all assumptions and caveats are revealed objectively so that meaningful comparisons can be performed, and to help point towards where improvements efficiently can be made.

3. Observations/Data Analyses

The observations are the only way to test if the models that have been developed in any way truly represent nature. However, the observations and analyses include a large set of assumptions. These include, for example, the physical limitations and calibrations of the instruments, the convection times of solar wind (for parameterization), location of the spacecraft within the magnetosheath relative to the boundaries, and many others. Below, each assumption is described in considerable detail.

3.1 Compilation of magnetosheath data sets

The method by which most researchers collect magnetosheath observation intervals is to examine time series of data, and locate the boundary (bow shock, magnetopause) locations. Spacecraft passes through the magnetosheath occur in three 'classes': 1) magnetopause -> bow shock or bow shock -> magnetopause, 2) magnetopause -> magnetopause, and 3) bow shock -> bow shock. The latter two 'classes' can be due to 'skimming' orbits, for which changes in the solar wind move the boundaries over

the spacecraft. Or, in the case of the second 'class', the spacecraft trajectory extends beyond the magnetopause, but does not reach the bow shock. A second, more automated method for identifying the magnetosheath region using the convected solar wind is to plot the magnetic field (normalized by solar wind magnetic field) against the ion density (normalized by the solar wind density). This will be discussed in more detail later.

In all cases, the spacecraft location with respect to the boundaries is only really 'known' at the boundary crossing itself. Within the magnetosheath proper, it is left to models parameterized by the solar wind condition to place the spacecraft with respect to the geophysical boundaries. Ideally, both plasma data and magnetic field observations are available to aid in the identification of the boundaries.

3.2 Compilation of solar wind data sets

Solar wind observations serve two functions with respect to observational studies of the magnetosheath. First, the solar wind observations are needed to determine whether discontinuities observed in the vicinity of the magnetosheath region correspond to the geophysical boundaries, or are discontinuities in the solar wind that are convected into the magnetosheath. Second, the solar wind observations are needed for parameterization of the magnetosheath condition as a function of the state of the solar wind. As with the magnetosheath data set, ideally both solar wind plasma moments and interplanetary magnetic field (IMF) data are important for use with the magnetosheath observations. The parameterization of magnetosheath observations according to the solar wind is complicated because the geophysical boundaries of the magnetosheath are affected differently by various parameters. For example, the magnetopause is most strongly affected by the solar wind dynamic pressure and the IMF B_z component (in GSM coordinates), while the bow shock location is most strongly affected by the solar wind magnetosonic Mach number, and the size/shape of the obstacle (the magnetopause). To further complicate matters, some researchers parameterize by either the Alfvén Mach number and/or the sonic Mach number. The Alfvén and sonic Mach numbers have their uses, as the sonic Mach number can be used to compare directly with original *Spreiter et al*. 1966 model results, and the Alfvén Mach number is useful for determining where stable reconnection occurs at the magnetopause, and may be useful for the reconnection rate. Plasma β (the ratio of thermal to magnetic pressures) also plays an important role.The different Mach numbers are related as follows:

$$M_{ms}^2 = 2/(1/M_A^2 + 1/M_s^2 + ((1/M_A^2 + 1/M_s^2)^2 - 4\cos^2\theta_{Bv}/(M_A^2 M_s^2))^{1/2})$$
$$= 2M_A^2/(1+\gamma\beta/2 + ((1+\gamma\beta/2)^2 - 2\gamma\beta\cos^2\theta_{Bv})^{1/2})$$
$$= \gamma\beta M_s^2/(1+\gamma\beta/2 + ((1+\gamma\beta/2)^2 - 2\gamma\beta\cos^2\theta_{Bv})^{1/2}),$$

and are all related to the solar wind dynamic pressure, since:

$$M_A^2 = \mu_0\rho v^2 / B_T^2, \quad M_s^2 = \rho v^2 / \gamma P_{Th}$$

In short, the state of the solar wind can be thought of in terms of 'coordinates' $\{M_{ms}, \beta\}$ or $\{M_A, M_s\}$. γ is the polytropic index. Additional factors such as the alpha particle content of the solar wind, and the flow direction are useful; though assumptions can be made if these parameters are not available.

Table 1. Summary table of important solar wind parameters

Parameter	Independent?	Useful for?	Comments
Proton Density	Yes (from dist. funct.)	Comparing with magnetosheath density; for dynamic pressure, plasma beta, and all Mach numbers	Some data sets cannot distinguish ion species; while others do.
Bulk Speed	Yes (from dist. funct.)	For estimating the solar wind convection time; comparing with magnetosheath velocity; for dynamic pressure, and all Mach numbers	Some solar wind data sets remove the Earth motion from the measured bulk speed (V_m = 29.8 km/s); some do not.
Proton Temperature	Yes (from dist. funct.)	Comparing with magnetosheath temperature; for plasma beta, sonic, and magnetosonic Mach numbers	Scalar value is used
Bulk Flow Direction (Angles)	Yes (from dist. funct.)	Aligning magnetosheath and magnetosphere with solar wind flow direction	If the flow direction is not available, then aberration angle = atan(V_m/V_{sw}) in the GSE equator is assumed. Often, a single value (e.g., 4°) is used. Beware of what angular conventions are used!
Alpha particle density	Yes (from dist. funct.)	For dynamic pressure, and all Mach numbers	If not available; a 4-5% by number (20-25% by mass) density is assumed.
Solar wind number flux	No; calculated from proton density and bulk speed	For comparing with magnetosheath number flux; Spreiter et al. model	
Solar wind dynamic pressure	No; calculated from ion (proton and alpha) density and bulk speed	For all Mach numbers; for normalizing the magnetopause location	For normalizing the magnetosheath Mach number by the solar wind Mach number, it is easy to disregard the alpha content in both quantities. But the alpha particle content is needed for normalizing the boundary locations

Sonic Mach number	No; calculated from ion density, bulk speed, and ion temperature	For comparing with magnetosheath sonic Mach number, Spreiter et al. model	A polytropic index must be assumed (usually 5/3)
Interplanetary magnetic field (IMF) intensity	Yes	For comparing with magnetosheath field intensity; for plasma beta, Alfvén Mach number and magnetosonic Mach number	
IMF components	Yes	IMF B_z (GSM): For normalizing the magnetopause location. IMF clock angle: For aid in identifying the magnetopause. IMF direction	IMF clock angle is generally conserved across the bow shock and into the magnetosheath, but not into the magnetosphere. It is not known if IMF B_z changes the bow shock location (southward IMF B_z reduces the magnetopause nose distance, but also creates a more blunt obstacle.)
Alfvén Mach number	No; calculated from ion density, bulk speed, and magnetic field intensity	For comparing with magnetosheath Alfven Mach number	
Ion plasma beta	No; calculated from ion density, ion temperature, and magnetic field intensity	For the triggering of plasma instabilities; may be useful for magnetopause reconnection rates	A polytropic index must be assumed (usually 5/3)
Magnetosonic Mach number	No; calculated from ion density, bulk speed, ion temperature, magnetic field intensity, and IMF components (direction angles)	For normalizing the bow shock location; for comparing with the magnetosheath magnetosonic Mach number	A polytropic index must be assumed (usually 5/3)

Just as there are times for which there are no solar wind observations (more on this below) to match with the magnetosheath samples, there are also times for which there are multiple spacecraft simultaneously observing the solar wind. Sometimes the different platforms observe very nearly the same solar wind values; but often the different platforms don't agree with one another or, for example, variations in the plasma and magnetic field are the same, but the relative timing of the changes differs from spacecraft to spacecraft (see Sec 3.4 (Convection times) below). The OMNI data sets do address this issue, but it is of continuing concern in all analyses which depend on the solar wind for parameterization.

3.3 Temporal coverage

For a variety of reasons (e.g., the mission is on-going), the time span of the magnetosheath data set will likely vary from study to study. This affects the spatial coverage and sampling, and can affect the spatial resolution. It is thus important to state not only the spacecraft data sets used, but the temporal coverage.

3.4 Convection times

Matching the convected state of the solar wind with spacecraft observations in other regions is a deceptively difficult task to do well. Many spacecraft are Earth-orbiting, and when these spacecraft sample the solar wind, they are usually situated just upstream of the bow shock. This is advantageous in that it is relatively easy to determine the convection time with small relative error (the typical solar wind travel speed is ~4 R_E/min). However, these spacecraft do not stay in the solar wind long, and so cannot be used for continuous monitoring. There are a few spacecraft that monitor the solar wind continuously; these reside in halo orbits around the L1 Lagrange point ~200 R_E upstream from the Earth. The disadvantages of monitoring the solar wind from this distance is that the relative error in the estimated convection time increases substantially. In addition, features observed in the solar wind near L1 can evolve spatially and temporally on their way to the near-Earth region. It is sometimes observed that simultaneous changes in the solar wind plasma and IMF at L1 are no longer simultaneous when observed close to the Earth. The simplest estimate for the convection time is simple $\Delta x/V_{sw}$, where Δx is the distance between the solar wind monitor and the point of interest, along the Sun-Earth line. More complex (and more accurate) estimates using minimum variance techniques and similar methods have been described in detail by *Weimer et al*., (2002, 2003), *Weimer* (2004), and others.

When the point of interest lies within the magnetosheath, then ideally the convection time including the time along the streamline through the magnetosheath should be performed in an iterative manner. That is, an initial estimate for the convection time would be used to determine contours of V/Vsw as well as the flow field within the magnetosheath, and then use this information to refine the convection time estimates, recalculate V/V_{sw} and the flow field, and repeat until the convection times remain fixed. A complicating issue is that if this exercise is performed for restricted sets of solar wind dynamic pressure or Mach number, then the sizes of these sets will change slightly from iteration to iteration, as the matching of convected solar wind to magnetosheath samples changes. However, this may be a small matter if the solar wind plasma parameters are slowly varying (or if there is a selection criterion for 'steadiness').

3.5 'Steadiness'

The issue of 'steadiness' is not a trivial one. For example, intervals for which the solar wind is unchanged for a long period are more forgiving with respect to the solar wind convection time

estimation. However, if the definition of 'steady' is restrictive, and if the magnetosheath sampling is filtered to only use 'steady' intervals (in order to model the 'steady state' magnetosheath), then there would be fewer magnetosheath samples which satisfy these criteria. This results in a smaller sampling set and more statistical uncertainty. Often, the definition of 'steady' is quantified as the standard deviation of a given parameter (sometimes normalized to its mean value) which is smaller than some value over a specified length of time and temporal resolution ($\sigma_p/<p> < value$). This assumes that the parameter follows a normal distribution (as is the case for components of the IMF, or the ion density (on a log scale); but is not usually the case for the bulk speed). The solar wind plasma parameters are often observed to be slowly varying and therefore fairly 'steady'; as compared to the varying direction of the IMF. Thus, the magnetosheath sampling set can quickly become vanishingly small if strict restrictions are placed on the long-time variations of multiple solar wind parameters.

A related issue concerning the solar wind measurements concerns the continuity of samples. Different data sets (e.g., plasma moments versus IMF) are sampled at different temporal resolutions, and are usually re-sampled to a common resolution. However, there are often gaps within one or more of the data sets. An issue then is how large of a data gap in a given solar wind variable is acceptable (and, to a lesser extent, how often do such gaps appear), when trying to match with the magnetosheath observations.

3.6 Defining the inner/outer boundaries of magnetosheath

The bow shock is easy to identify in observations as near step-function changes in the plasma moments and magnetic field intensity. The bow shock satisfies well the Rankine-Hugoniot relations across a discontinuity, though there sometimes exists a shock foot and/or an overshoot. The magnetopause can be more difficult to identify. Typically, the magnetopause is demarked as the start of the magnetic field rotation from magnetosheath field towards the magnetospheric field. However, the magnetopause determination can be complicated because of the presence of boundary layers. It can also be complicated because the magnetopause location is a boundary defined by pressure balance, and there are times when the component pressures on both sides of the magnetopause are nearly equal. A typical example of the bow shock and magnetopause crossings are shown in Figure1.

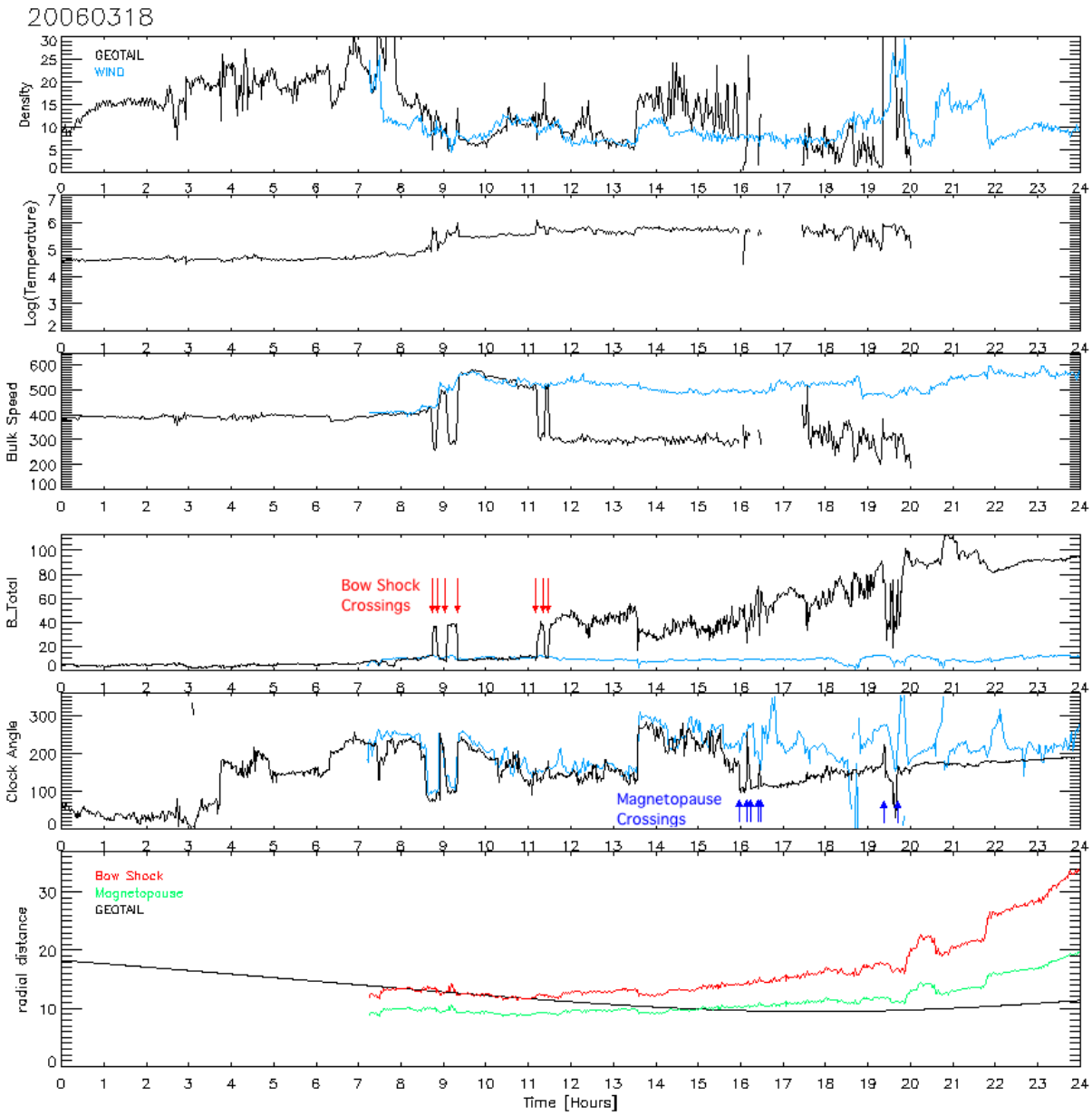

Fig.1. An example time series showing Geotail bow shock and magnetopause crossings. Solar wind data is convected by 30 minutes.

A more automated procedure to select magnetosheath intervals from spacecraft observations has been employed by *Jelinek et al*. This method plots the density ratio (n/n_{sw}) against the magnetic field ratio (B/B_{sw}). When both ratios are close to unity, the sampling spacecraft is in the solar wind. When the density ratio is very small, the sampling spacecraft is in the magnetosphere (MS). An example of this selection process on spacecraft observations is shown in Figure 2.

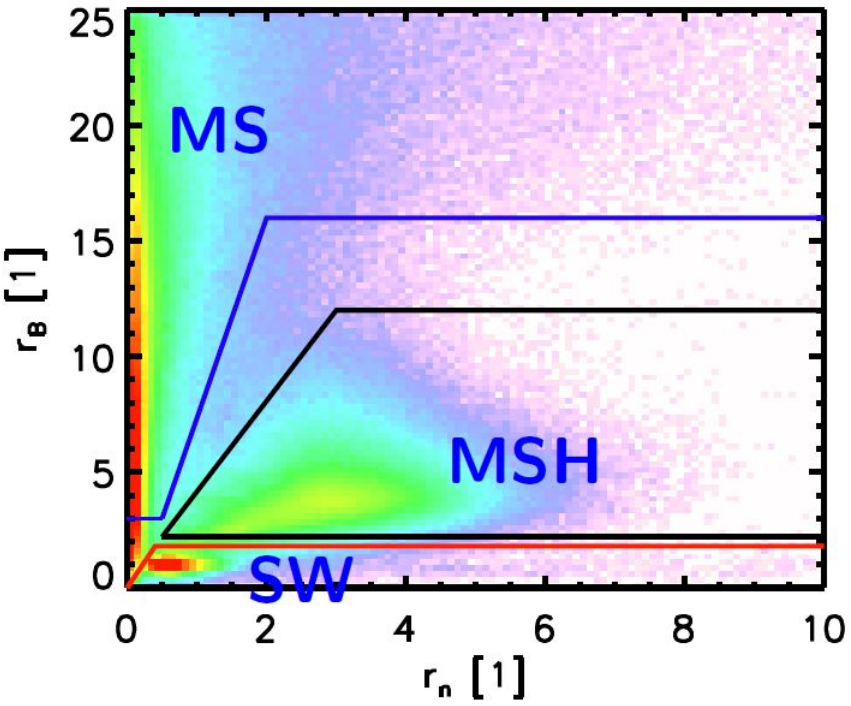

Fig. 2. An example from *Jelinek et al*. (COSPAR 2010 presentation) of automatic selection of THEMIS magnetosheath sampling intervals (MSH); displaying a 2D histogram of the magnetic field ratio ($r_B = B/B_{sw}$) with the density ratio ($r_n = n/n_{sw}$). Solar wind values are from ACE.

3.7 Towards the creation of synoptic maps

Once the magnetosheath intervals have been identified and the samples are matched with the solar wind condition, the next step often taken is to create synoptic maps of the magnetosheath region. There are several factors which must be considered in this process; many of which are related to spatial coverage.

3.7.1 Normalization techniques with empirical models

Although the geophysical boundaries are persistent 'standing' discontinuities (except in very rare cases when the solar wind magnetosonic Mach number dips below unity and the bow shock temporarily disappears), the boundaries move about average locations. In order to create synoptic maps of the magnetosheath with sharply defined inner and outer boundaries, the locations at which observations are made are often 'normalized' so as to fit between the defined boundaries. Existing empirical models of the bow shock and magnetopause and their dependence on the solar wind condition are often employed to normalize the sampling location in space relative to the boundaries (an alternative strategy is to use small subsets of the observations with restricted ranges of the solar wind parameters, and forego any normalization of the sampling locations). For example, Verigin *et al*., (2006) calculated the fractional distance between a given magnetosheath data point and model magnetopause and bow

shock locations, and presented a spatial distribution of mirror mode waves in a coordinate system where the vertical axis is the fractional distance and the horizontal axis is the zenith angle in magnetosheath-interplanetary medium reference frame.

The boundary models themselves are often crude fits to boundary observations, and so the normalization is found to be imprecise. Specifically, magnetosheath observations not within the model magnetosheath region may still lie outside the model region even after normalization. Even observations initially within the model region may fall outside the region after normalization. Two options are then to 're-normalize' the observations, forcing each magnetosheath pass to match the boundaries at the entry/exit points, or to simply ignore the observations which lie outside the model boundaries (since these may be due to dynamic solar wind conditions or other transients).

3.7.2 Spatial coverage: Symmetries, and data folding

Sparse sampling of the magnetosheath, especially when filtered for certain solar wind conditions, often provides motivation towards taking advantage of assumed symmetries to fold the data sets, thereby increasing the statistical significance of the sampled regions.

3.7.2.1 Full 3D modeling

The magnetosheath volume is very large (~10^4 R_E^3 on the dayside alone). Despite the numerous missions which have traversed the magnetosheath over the decades, the spatial sampling in the full 3D region is in fact rather sparse. For data analysis and parameterization of the magnetosheath properties according to the solar wind condition, it is usually best to assume some symmetry exists, and the observations are then rotated or projected into a smaller (usually 2D) region. This has the advantage of increasing the independent samples and the associated statistics. Depending on the assumptions of symmetry and boundary models, if one normalizes the observation locations, it may either be performed before or after rotating/projecting into the smaller region.

3.7.2.2 High/low latitudes

Some empirical models of the magnetopause have shown that the shape of this boundary is different at low versus high latitudes (e.g., *Sibeck et al*., 1991; *Boardsen et al*., 2000). The reason for this difference may be due to the cusps, though Region 1 currents may also play a role. Many models do not make a distinction in shape as a function of latitude (e.g., *Tsyganenko*, 1995; *Shue et al*., 1997, 1998). It is also not clear if the bow shock shape varies as a function of latitude; spacecraft do not usually cross the high-latitude bow shock (though Cluster was able to reach the bow shock at up to ~65° latitude). Most observations of the magnetosheath occur at low-latitudes, and so the low-latitude boundary shapes are appropriate most of the time. However, this is a potential issue for observational studies and for model development.

3.7.2.3 Mapping of data into planes

In order to display magnetosheath (contours or vector plots), a 2D plane is usually chosen. The plane is usually either the equatorial plane or a noon-midnight meridian plane (in either GSE or GSM

coordinates). Since the observations do not occur in exactly these planes, the observations which are close to these planes are projected by some manner into the plane. There are two ways by which this is accomplished: 1) Rotation: Observations occurring within a specified angle of a plane of interest are rotated into that plane, about an axis that contains the solar wind velocity vector, and 2) $\Delta Z'$: Observations occurring within some small distance ($\pm Z'$) from a plane of interest are projected linearly into that plane.

3.7.2.4 Folding of data

Due to limited spatial coverage by spacecraft of the 3D region of the magnetosheath, many observational studies increase the statistical significance by taking advantage of the assumed symmetry of the magnetosheath and 'folding' the sampling points, even after mapping into a plane. This is usually accomplished by, e.g., mapping dawn and dusk samples into a single half-plane, or mapping samples north/south of the equator into a single half-plane. The IMF direction should also be considered in the folding. One complicating factor is that the geophysical boundaries may depend on the IMF direction, such as the change in the magnetopause shape by IMF B_z. While folding increases the number of samples within spatial bins, processes which exhibit a directional preference within the magnetosheath may not be discerned.

3.7.3 Spatial coverage: Resolution and parameter ranges

In addition to any mapping and/or folding of the data sets, the spacecraft observations may be categorized according to the solar wind conditions, and spatially binned. Choosing larger spatial bins will increase the number of samples per bin, but may cause misleading results in regions where significant gradients in the plasma properties exist. This issue also involves the implicit assumptions to be made as to the coherence time of the solar wind and magnetosheath, and to the statistical independence of the samples.

3.7.4 Coordinate systems

Various coordinate systems have been used over the years in the different models. On the one hand, simple Cartesian grids are easiest to work with. On the other hand, for analytic models it is often most convenient to use a coordinate system with surfaces which matches the boundaries. In any case, in order to model the magnetosheath region, it is usually best to choose a single, orthogonal coordinate system which works well at both boundaries. In terms of the resulting contour plots and large scale variations, a robust statistical sampling should be independent of the coordinate system used, with the possible exception of the regions near the boundaries. Due to the strong variations of parameters and the relative closeness of the bow shock and magnetopause along the stagnation streamline, it is generally a good strategy to use small spatial bins in this region. In the tail flank regions, larger bins are preferred, since the parameter variations are more gradual, and because the sampling is more sparse. Below we briefly discuss several of these coordinate systems.

3.7.4.1 Cubic/rectangular grid

The easiest coordinate system to work with, but may not be the optimum for modeling purposes. This assessment depends on the sampling statistics and expected spatial gradients; especially close to the boundaries.

3.7.4.2 Spherical/polar grid

This coordinate system is usually designed to take advantage of the symmetry about the solar wind flow direction, such that the polar axis is aligned with the solar wind flow. Bins are defined as surfaces of constant radius and constant polar angle (θ). Usually the center of the spherical coordinate system is co-located with the Earth center; but this need not be the case. If the radial surfaces are equally spaced (e.g., 10 < r < 11 R_E, 11 < r < 12 R_E, etc.), the bins at smaller radii are smaller than those at larger radii, and thus may not be sufficiently sampled.

3.7.4.3 Ellipsoidal (prolate spheroid)/elliptical grid

The elliptical coordinate system was used by *Tsyganenko* (1989) to describe an analytic vacuum magnetospheric magnetic field model. *Farris et al*. (1991) and *Petrinec and Russell* (1993); used ellipsoids (with Earth centered at one focus) to empirically fit the dayside bow shock and magnetopause shapes, respectively. Different ellipsoidal shapes (i.e., diffferent eccentricities) are used to fit the bow shock and magnetopause. As with the sperical coordinate system, the ellipsoidal coordinates are chosen so that the major axis aligns with the solar wind flow direction.

3.7.4.4 Paraboloidal/parabolic grid

The origin of this coordinate system is usually taken as one focus of the paraboloid and may lie at the center of the Earth (e.g., *Stern*, 1985), half-way between the Earth and boundaries (e.g., *Kobel and Flückiger* [1994]; *Romashets et al.* [2008]), or some other location. While paraboloidal model fits are fairly reasonable for models of the magnetopause, the use for the bow shock is more questionable, as the bow shock shape tends to lie much closer to the magnetopause in the flank regions than is observed.

3.7.4.5 Other orthogonal coordinate systems; alignment with geophysical boundaries

Many empirical models of the magnetopause and bow shock boundaries have used simple conic sections, with the various coefficients parameterized to the solar wind condition as determined from fits to the observed boundary locations. However, the current most often used empirical magnetopause model (*Shue et al*., 1998) does not conform to any simple conic section (though it derives from a parabolic function with the Earth at the focus). Specifically, the representative function is $r = r_0(2/(1+\cos\theta))^{\alpha}$. $\alpha = 1$ would represent a paraboloid, whereas in the *Shue et al*. model, $\alpha = \alpha(\rho v^2_{sw}$, IMF $B_{z\text{-}GSM}$). This is certainly acceptable, though as a coordinate system it is not the easiest system in which to work.

As with the *Shue et al*. magnetopause model, *Chao et al*. 2002 have used an analogous method to create a functional form to represent the bow shock, as a function of solar wind parameters.

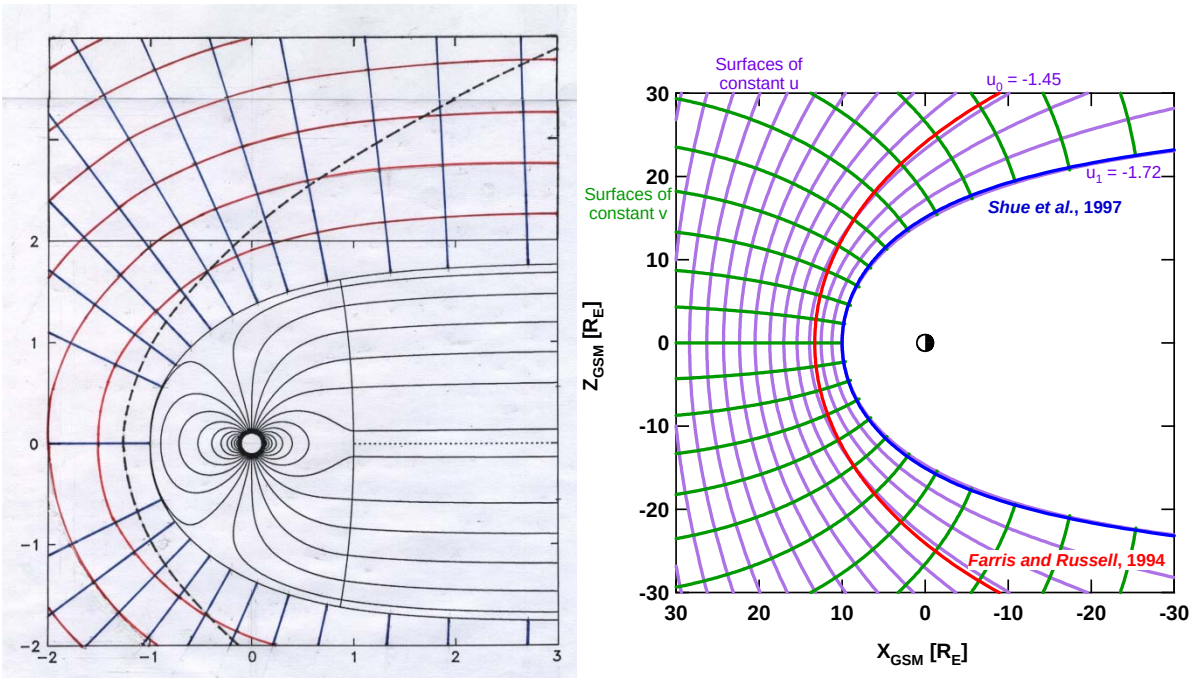

Fig. 3 Other coordinate systems are being investigated by M.Schulz and M.Chen (left) and by S.M.Petrinec (right).

3.7.5 Determined values for spatial bins

If the parameters studied are well-behaved and Gaussian in nature, then the mean and median values of such parameters determined in each spatial bin of the magnetosheath should be close to one another. However, in many cases the distributions are not Gaussian, or are better distributed in logarithmic space. It is important to note what values (e.g., mean, median) are determined (and plotted) for a given synoptic map. All observation-based synoptic maps entered into the library data base should also include maps of the variances and of the sampling.

4. Numerical Models

As the geospace occupies a very large volume (~300×80×80 R_E^3) and because it also contains many smaller-scale structures such as the magnetopause and associated boundary layers, shocks and reconnection X-lines where the physical length scales approach ion and electron scales, the accurate modeling of this region is a computational challenge. In order to capture the physics of each region one typically needs at least 10 gridpoints/physical length scale. Resolving well a current layer that is 600 km thick would require a minimum resolution of ~60 km^3, or 0.0094 R_E^3. Utilizing this resolution for the entire volume would require about 200 million grid points. Resolving an ion inertial scale, c/ω_{pi}, of 100 km would require a resolution of 10 km. Hence, resolving and electron physics at the reconnection X-line would require even larger resolution (by a factor of $\sqrt{1/1836}$ c/ω_{pi}). So it is clear that with current computer resources it is impossible to model the entire volume at the highest resolution.

Additionally, a fully kinetic 3-D global approach with realistic electron to ion mass ratios is not computationally feasible. In the hybrid approach, ions are treated as particles but the electrons are treated as a fluid (cf., *Winske and Omidi*, 1996). This method has now reached a developmental stage where at least small bodies (e.g., the Moon, Mercury) can be modeled globally; however, global hybrid simulations of the Earth with realistic parameters are probably still a few years away [*J. Raeder*, 2006].

The most basic fluid treatment that allows the construction of global models is magnetohydrodynamics (MHD). Careful consideration of the conditions under which MHD is derived shows that many of these conditions are violated in geospace. However, the MHD equations are the basic conservation equations for mass, momentum, energy, and magnetic flux, and thus describe at least the convective transport correctly. One of the primary simplifications of MHD is the truncation of the moment equations at the second moment (pressure). However, if the distributions of the particles are Maxwellian the higher moments vanish. Fortunately, in many regions of geospace the distribution functions stay close to Maxwellian because of waves and turbulence and thus the MHD closure of the moment equations is not a bad approximation [*J. Raeder*, 2006].

The local models have a finite domain size and in these the fully kinetic simulations are possible. One disadvantage of the local simulations, however, is the unrealistic boundary conditions. These are extremely useful for studying the instabilities and physics that the global codes cannot address.

In the following we will briefly discuss the limitations of the various models and what kind of things need to be considered when these models are used for magnetosheath modeling.

4.1 Global MHD models

For ideal MHD there is no intrinsic physical length scale and the system can be considered self-similar. The characteristic time scale is defined by the Alfvén wave travel time through system length scale: if the system size is doubled, the time scale doubles. However, in ideal MHD reconnection is not possible, so if one wants to include a dissipation mechanism, resistive MHD is the numerically least expensive way to go. Because the numerical diffusion of the codes depends on the used grid resolution, even ideal MHD would produce diffusion in global codes. However, in this approach reconnection is a random process and has nothing to do with physical reconnection.

A typical approach is to use current dependent resistivity; so reconnection is initiated when a certain threshold current is reached at the current layer. However, this method is not applicable in the low plasma resistivity limit. The Petschek reconnection mechanism is only relevant when the plasma resistivity is spatially localized in such a way that the spatial scale of the current layer is proportional to the magnitude of the resistivity. Without such spatial localization (e.g., if the plasma resistivity is spatially uniform), reconnection is typically observed to occur in long, thin Sweet-Parker current sheets [*Sweet*, 1958; *Parker*, 1957].

The MHD approximation can be further improved by taking into account more terms in Generalized Ohm's law. Measuring all quantities in typical units, the coefficients of the different terms in Ohm's law can be determined. If the electron inertia terms (c/ω_{pe}) are neglected, the corresponding set of equations are often referred to as Hall MHD. If both electron and ion inertia terms are neglected then Ohm's law is called resistive Ohm's law and the MHD equations are referred to as resistive MHD. If the resistivity is assumed to be zero, this is 'ideal' MHD.

Currently there are four global physics based MHD models (BATSRUS, Open GGCM, Gumics and LFM) available for community use at the Community Coordinated Modeling Center, hosted at the NASA Goddard Space Flight Center (http://ccmc.gsfc.nasa.gov/models/models_at_glance.php). Some of these use an adaptive grid, so higher resolution can be used in regions of interest such as the magnetopause. Currently the highest available standard resolution for 'Runs on Request' is ¼ R_E, but the CCMC team is very helpful and can increase the resolution up to 1/16 R_E when necessary, which corresponds to resolution of ~400 km, and suggests that structures with a 2000-4000 km length scale would be well resolved.

While the magnetosheath region along the Sun-Earth line is typically of a thickness of 3-7 R_E (depending on the solar wind dynamic pressure, sonic Mach number, Alfvén Mach number and the angle between solar wind magnetic field and velocity vector (cf., *Verigin et al.* 2006)), and as such seems to be of a scale size well-suited for global MHD modeling using the CCMC models, there are several issues for which one needs to be made aware.

For example, *Dorelli et al*., 2004 performed several simulations in the limiting case of high-Lundqvist number, S (where S is the dimensionless ratio of an Alfvén wave crossing timescale to a resistive diffusion timescale) and found that:

1. When the plasma resistivity is constant (i.e., not current-dependent or spatially localized), driven subsolar reconnection occurs in thin current sheets of macroscopic length, rather than in Petschek-like configurations where slow shocks play a dominant role in the magnetic dissipation and plasma acceleration processes.
2. Magnetic energy builds up outside the current sheet to accommodate the magnetosheath flow.
3. The scaling of magnetic pileup with Lundquist number observed in the MHD simulations is consistent with that predicted by the three-dimensional analytical stagnation point flow solutions of the resistive MHD equation. The reconnection electric field upstream of the current sheet scales as $1/S^{0.2}$. Thus, the reconnection rate vanishes in the limit S-> ∞. That is, without anomalous resistivity, which can enhance the reconnection rate either by decreasing S or spatially localizing it, global MHD simulations will likely not reproduce Dungey's open magnetosphere for large values of S.

To solve the reconnection timescale problem, *Dorelli et al.* 2004, suggest the following approaches:

- Seek solutions of the resistive MHD equations such that the reconnection rate is insensitive to the Lundquist number
- Take into account additional terms in the generalized Ohm's law to take into account kinetic scale physics which are neglected in the ideal/resistive MHD. For example the GEM Reconnection Challenge demonstrated that Hall electric fields permit ''fast'' (i.e., on Alfvénic timescales) reconnection to occur independently of the dissipation mechanism (*Birn et al.* 2001), which suggest that global Hall-MHD would get the reconnection rate right, avoid the timescale problem, and would be numerically the 'least challenging' improvement.

With regard to magnetosheath modeling, the issue is that the current global codes might yield a subsolar magnetosheath with unrealistic high magnetic flux pile up and thus there would be a discrepancy between magnetosheath observations such as plasma β when compared to model results; especially in high Lundkvist number limit.

It is important that in addition to the MHD approximation used (current dependent localized resistivity, uniform resistivity, Hall-MHD with electron pressure term, Hall-MHD without electron pressure term, or two-fluid) a header file describing a numerical simulation includes information on the parameter regime (Lundkvist number) and grid resolution of the run.

Another limitation of the MHD approach is the lack of kinetic physics that plays a role within the magnetosheath and at the boundaries. For example, mirror-mode fluctuations cannot be captured in MHD. In the reconnection process and at the shock, non-Maxwellian distributions are observed, but are not captured in MHD models.

4.2 Global hybrid models

Global hybrid simulations provide a collective picture of processes taking place in the foreshock, bow shock, and magnetosheath. In the hybrid codes, electrons are treated as a massless fluid and ions are treated kinetically by Particle-In-Cell (PIC) methods. Because ions are treated as particles, these codes also give information on ion-scale microphysics. Since magnetosheath properties depend on the solar wind and shock physics and *in situ* magnetosheath processes, it is clear that the global hybrid simulations would better capture the detailed physics of the magnetosheath region than the global MHD models. The first self-consistent 2-D global hybrid simulations of the bow-shock, magnetosheath and dayside reconnection region first appeared 11 years ago (L. Yin, 2001).

X. Blaco-Cano *et al*., 2006 reproduced a variety of low-frequency waves (ion cyclotron, mirror, magnetosonic, mixture of magnetosonic modes) downstream from the bow shock in the magnetosheath plasma, using 2-D global hybrid simulations. While some of these waves are produced locally, others may result from shock mode conversion of upstream waves. It is clear that the waves have a macroscopic effect on the ambient magnetosheath plasma. In 2009, X. Blanco-Cano *et al*. simulated with a global 2-D hybrid model weakly compressive ultralow frequency (ULF) waves permeating the foreshock region; including density cavitons that are bounded by enhanced magnetic fields, and hot diffuse ions present within them. Cavitons are important because they are carried by the solar wind through the bow shock where their properties may evolve, leading to large density pulses within the magnetosheath that can cause surface waves at the magnetopause .

The maximum domain size in 2-D glocal hybrid simulations (*Blanco-Cano et al*. 2006) is typically 1200x1600 c/ω_{pi}, which is about 50 times smaller than the system size in global MHD simulations (300 R_E x 80 R_E) assuming an average ion inertial length of 100 km. For example, the subsolar magnetosheath thickness in Figure 4 is ~120 c/ω_{pi}, corresponding to ~12000 km (~1.9 R_E) and thus underestimates by a factor of ~2 the typical observed magnetosheath thickness. This difference may overestimate the influence of the ion-inertial scale physics on the global magnetosheath and magnetospheric dynamics.

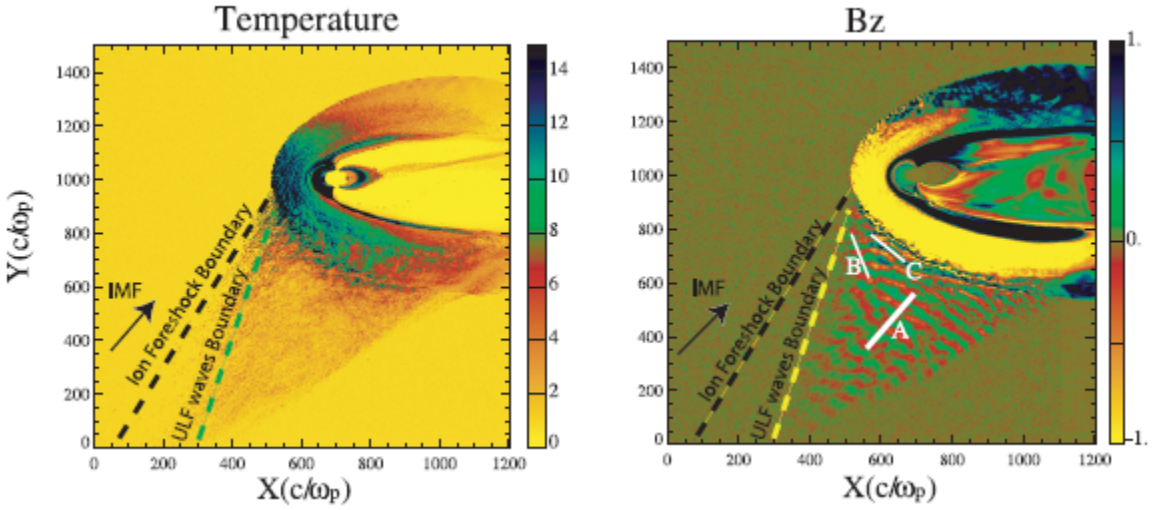

Fig4. Temperature and B_z in a 2-D global hybrid simulation by *Blanco-Cano et al*. 2006.

Another limitation of current hybrid models is their two-dimensional nature. Spacecraft observations have shown that the magnetosheath has complex 3-D structure with full asymmetry. It is therefore desired that full 3-D global hybrid simulations would be developed using realistic domain sizes in pertinent regions. For magnetosheath purposes it is not necessary to model the entire magnetotail region. Semi-global 3-D hybrid simulations with realistic scales and reaonable run-times are likely to be feasible in the very near future.

4.3 PIC and global and local kinetic models

Although global kinetic-scale self-consistent magnetospheric simulations are not currently feasible, there presently exists global MHD models that follow several millions of test particles in MHD fields to study particle motion from the solar wind into the magnetosphere.

The local kinetic codes can be used for studying *in situ* magnetosheath physics such as reconnection in thin current sheets and wave particle interactions within the magnetosheath.

5. Analytic/Theoretical Models

Analytic models of the plasma parameters and magnetic field of the steady-state magnetosheath are important for providing a relatively simple-to-use method for estimating baseline or ambient values at specific locations within the magnetosheath. It is understood that these models are meant to represent quantities at a zeroth-order level, and that plasma instabilities and kinetic phenomena cannot readily be described with such models. The analytic models for the magnetosheath are expected to be analogous to the Tsyganenko magnetospheric field models which provide a baseline characterization of the space environment (i.e., magnetic field) interior to the magnetopause boundary. A significant reason for the difficulty with the development of such analytic magnetosheath models is that the magnetic field

and the plasma moments are intertwined; as exemplified by Rankine-Hugoniot conditions across the bow shock, or by **J**x**B** forces within the magnetosheath. Therefore, a robust analytic magnetosheath magnetic field model really needs to be characterized by the solar wind plasma condition (in addition to the IMF), and a robust plasma moment model should be characterized by the IMF condition (in addition to the upstream plasma moments).

5.1 Plasma moment models

There have been rather few analytic models which describe the global magnetosheath plasma moments. The pioneering work of *Spreiter et al*. [1966] used a gas-dynamic approach with an embedded magnetic field, rather than an MHD method. Although analytic forms of the magnetosheath plasma moments were not explicitly provided, contour maps were created which continue to be extremely valuable to many studies as a baseline estimate for the ion density, bulk velocity, mass flux, temperature, and sonic Mach number throughout the magnetosheath. These contour maps, however, are independent of the IMF.

The derivations of J.Spreiter also provided analytic formulations of plasma moments along the stagnation streamline, which lies closest to the magnetopause. These are most appropriate for the very special case of the IMF aligned along the solar wind flow direction. For other IMF directions, significant discrepancies may result. Analytic forms for the plasma moments along the magnetopause have been provided by *Petrinec and Russell* [1997] and *Cooling* [2001]. These analytic formulations, however, suffer from several other deficiencies for modeling the real plasma properties. Among these are that they are only of use very close to the magnetopause, and yet they do not account for the plasma depletion layer, magnetosheath boundary layer, reconnection flows, etc. (e.g., *Zwan and Wolf* [1976]). In addition, **J**x**B** and ∇P forces are a significant influence on the plasma parameters not only near the magnetopause, but throughout the magnetosheath (e.g., *Petrinec et al*., 1997; *Lavraud et al*., 2007).

5.2 Magnetic field models

Analytic models of the magnetosheath magnetic field are extremely useful for estimating the draping of the shocked IMF around the magnetosphere, which is then used to help determine where magnetopause reconnection is likely to occur (both directly by nature of the magnetic shear angle across the magnetopause, and indirectly via the plasma β and Alfvén Mach number). Some relatively recent models which provide analytic solutions for the magnetic field of the magnetosheath are those of *Kobel and Flückiger* [1994] and *Romashets* [2008]. These models solve for the scalar magnetic potential and the vector potential of the magnetosheath, respectively. Both use boundary conditions at the bow shock and magnetopause in the development of the solution, and both models are expressed as a function of the IMF. In addition, as described in Section 3.7.4.4, both models also use paraboloids for the bow shock and magnetopause. This choice of boundary shapes simplifies the mathematics considerably. However, the shapes do not approximate well the observed shapes of the boundaries, especially in the flank regions. Thus, in order to use the models to compare with observations and/or with other models

(for example, in conjunction with the Tsyganenko models), the user must perform some kind of conformal mapping of the boundary shapes and of the magnetic field. This can be performed in more than one way; e.g., stretching/compressing the component along the axial symmetry axis to match another known boundary like the *Shue et al*. magnetopause; or mapping along the boundary normals to force the boundaries to coincide.

6. GEM Magnetosheath Focus Group Challenge

The Geospace Environment Modeling Magnetosheath Focus Group Challenge is to compare and contrast synoptic maps of the magnetosheath for specific parameter ranges of the solar wind conditions, as produced from data sets and from numerical models. It may also be possible that simple analytic models can be created which adequately describe the parameter variations of the magnetosheath as produced by the observational and numerical model maps.

6.1 Challenge details

Synoptic maps of the magnetosheath region are to be created subject to the following sets of input constraints:

1) Two magnetic field configurations: Parker-spiral orientation; ortho-Parker-spiral orientation of the IMF (with IMF B_x and IMF B_y each > 0.4 B_{Total}).

2) 'Steady-state' definition: 20 minutes steady with low standard deviation.

3) Magnetosonic Mach number ranges for data: ($1<M_{ms}<3$; $3<M_{ms}< 7$; $7<M_{ms}< 10$; $10<M_{ms}<14$)

4) Plasma β:

- Ranges for observations: ($0.01<\beta<0.2$; $0.2<\beta<2$; $2<\beta<6$; $6<\beta<12$)
- Numerical models: (β=0.1, 1, 10)

Output parameters to be studied:

- Plasma moments
- Temperature anisotropies, pressure anisotropies
- Electron/ion temperature ratios
- Wave power and wave modes spectra in magnetic field and velocity-field fluctuations, density fluctuations, pressure fluctuations, specific entropy

Also of specific interest at the magnetopause is the variation of the magnetosheath Alfvén Mach number. This is important for determining over what region stable magnetic reconnection is able to take place, and may also be important for quantifying the reconnection rate.

6.2 Metrics

Metrics (i.e., quantitative assessments of individual maps under given sets of solar wind conditions) are important for determining how closely various models compare with one another, and may point towards where improvements should be made. A simple yet effective strategy would be to provide a single 'score' for a given map comparison. Such a score may be based upon a χ-squared calculation over the entire magnetosheath region; perhaps with a prescribed (stronger) weighting near the geophysical boundaries and near the subsolar region. Comparisons between observational and numerical models may be complicated by the shapes of the boundaries used, as well as the coordinate systems and spatial resolutions used. Normalization and interpolation may need to be employed for some comparisons. Comparisons should also be recorded in the library, with a detailed description as to how the procedure was performed. Comparisons with analytic models should be somewhat easier, as the spatial resolution should not be a factor in analytic models.

7. References

Birn, J., *et al*. (2001), Geospace Environmental Modeling (GEM) Magnetic Reconnection Challenge*, J. Geophys. Res., 106(A3)*, 3715–3719, doi:10.1029/1999JA900449.

Blanco-Cano, X., N. Omidi, and C.T. Russell (2006), Macrostructure of collisionless bow shocks: 2. ULF waves in the foreshock and magnetosheath, *J. Geophys. Res., 111*, A10205, doi:10.1029/2005JA011421.

Boardsen, S.A., T.E. Eastman, T. Sotirelis, and J.L. Green (2000), An empirical model of the high-latitude magnetopause, *J. Geophys. Res., 105(A10)*, 23193–23219, doi:10.1029/1998JA000143.

Chao, J.K., D.J. Wu, C.-H. Lin, Y.-H. Yang, X.Y. Wang, M. Kessel, S.H. Chen, and R.P. Lepping (2002), Models for the size and shape of the Earth's magnetopause and bow shock,

Cooling, B. M. A., C. J. Owen, and S. J. Schwartz (2001), Role of the magnetosheath flow in determining the motion of open flux tubes, *J. Geophys. Res., 106*, 18763.

Dorelli, J.C., M. Hesse, M.M. Kuznetsova, L. Rastaetter, and J. Raeder (2004), A new look at driven magnetic reconnection at the terrestrial subsolar magnetopause, *J. Geophys. Res., 109*, A12216, doi:10.1029/2004JA010458.

Farris, M., S. M. Petrinec, and C. T. Russell (1991), The thickness of the magnetosheath: Constraints on the polytropic index, *Geophys. Res. Lett., 18*, 1821-1824.

Kobel, E. and E.O. Flückiger (1994), A model of the steady state magnetic field in the magnetosheath, *J. Geophys. Res., 99*, 23617-23622.

Lavraud, B., J.E. Borovsky, A.J. Ridley, E.W. Pogue, M.F. Thomsen, H. Rème, A.N. Fazakerley, and E.A. Lucek (2007), Strong bulk plasma acceleration in Earth's magnetosheath: A magnetic slingshot effect?, *Geophys. Res. Lett., 34*, doi:10.1029/2007GL030024.

Parker, E. N. (1957), Sweet's mechanism for merging magnetic fields in conducting fluids, *J. Geophys. Res.*, 62(4), 509–520, doi:10.1029/JZ062i004p00509.

Petrinec, S.M. and C.T. Russell (1993), External and internal influences on the size of the dayside terrestrial magnetosphere, *Geophys. Res. Lett., 20*, 339-342.

Petrinec, S.M. and C.T. Russell (1997), Hydrodynamic and MHD equations across the bow shock and along the surfaces of planetary obstacles, *Space Sci. Rev., 79*, 757-791.

Petrinec, S. M., T. Mukai, A. Nishida, T. Yamamoto, T. K. Nakamura, and S. Kokubun (1997), Geotail observations of magnetosheath flow near the magnetopause, using Wind as a solar wind monitor, *J. Geophys. Res., 102(A12)*, 26,943–26,959, doi:10.1029/97JA01637

Romashets, E.P., S. Poedts, and M. Vandas (2008), Modeling the magnetic field in the magnetosheath region, *J. Geophys. Res., 113*, doi:10.1029/2006JA012072.

Shue, J.-H., J.K. Chao, H.C. Fu, C.T. Russell, P. Song, K.K. Khurana, and H.J. Singer (1997), A new functional form to study the solar wind control of the magnetopause size and shape, *J. Geophys. Res., 102(A5)*, 9497–9511, doi:10.1029/97JA00196.

Shue, J.-H., P. Song, C.T. Russell, J.T. Steinberg, J.K. Chao, G. Zastenker, O.L. Vaisberg, S. Kokubun, H.J. Singer, T.R. Detman, H. Kawano (1998), Magnetopause location under extreme solar wind conditions, *J. Geophys. Res., 103*, 17691–17700, doi:10.1029/98JA01103.

Sibeck, D.G, R.E. Lopez, and E.C. Roelof (1991), Solar wind control of the magnetopause shape, location, and motion, *J. Geophys. Res., 96*, 5489.

Spreiter, J.R., A.L. Summers, and A.Y. Alksne (1966), Hydromagnetic flow around the magnetosphere, *Planet. Space Sci., 14*, 223.

Stern, D.P. (1985), Parabolic harmonics in magnetospheric modeling: The main dipole and the ring current, *J. Geophys. Res., 90(A11)*, 10851–10863, doi:10.1029/JA090iA11p10851.

Sweet, P.A. (1958), The neutral point theory of solar flares, IAU Symposium No. 6, Electromagnetic Phenomena in Ionized Gases (Stockholm 1956), p.123.

Tsyganenko, N.A. (1989), A solution of the Chapman-Ferraro problem for an ellipsoidal magnetopause *Planet. Space Sci., 37*, 1037.

Tsyganenko, N.A. (1995), Modeling the Earth's magnetospheric magnetic field confined within a realistic magnetopause, *J. Geophys. Res., 100*, 5599.

Verigin, M.I., M. Tátrallyay, G. Erdős, and G.A. Kotova (2006), *Adv. Space Res., 37*, 515–521.

Weimer, D. R., D. M. Ober, N. C. Maynard,W. J. Burke, M. R. Collier, D. J. McComas, N. F. Ness, and C. W. Smith (2002), Variable time delays in the propagation of the interplanetary magnetic field, J. Geophys. Res., 107(A8), 1210, doi:10.1029/2001JA009102.

Weimer, D. R., D. M. Ober, N. C. Maynard, M. R. Collier, D. J. McComas, N. F. Ness, C. W. Smith, and J. Watermann (2003), Predicting interplanetary magnetic field (IMF) propagation delay times using the minimum variance technique, J. Geophys. Res., 108(A1), 1026, doi:10.1029/2002JA009405.

Weimer, D. R. (2004), Correction to "Predicting interplanetary magnetic field (IMF) propagation delay times using the minimum variance technique," *J. Geophys. Res., 109*, A12104, doi:10.1029/2004JA010691.

Winske, D., and N. Omidi (1996), A nonspecialist's guide to kinetic simulations of space plasmas, *J. Geophys. Res., 101(A8)*, 17287–17303, doi:10.1029/96JA00982.

Zwan, B.J., and R.A. Wolf (1976), Depletion of solar wind plasma near a planetary boundary, *J. Geophys. Res., 81(10)*, 1636–1648, doi:10.1029/JA081i010p01636.

8. Appendix

The following is an example of a header file for an observations-based magnetosheath model:

Parameter	Value(s)	Comments
Model type	Empirical	
Magnetosheath data sets used	Geotail	7/1992 – 12/2011
Solar wind data sets used	IMP-8, Wind, ACE	
Parameter(s) examined	Ion plasma moments	n_i, v_i, T_i
Acceptable solar wind temporal data gap size	5 min	
Convection time determination	Weimer et al. 2003 model	Direction of min. variance in a plane orthogonal to the mean field
Time resolution of magnetosheath data set	5 min	Coherence time is assumed to be ≤ 5 min
Normalization technique	Scaling between boundaries	Scale magnetosheath passes to fit between model bow shock and model magnetopause
Magnetopause model used for normalization	*Shue et al*., 1998	
Bow shock model used for normalization	*Farris and Russell*, 1994	
Magnetosheath coordinate system	Aberrated GSM coordinates, Spherical	Geocentric, θ=0° polar direction along anti-solar wind direction, ϕ=0° azimuthal direction along +Y-axis, increasing towards +Z-axis.
Spatial resolution	$\Delta r = .25\ R_E$, $\Delta\theta = 5°$	
Folding of data	Rotated into GSM-equatorial plane	All magnetosheath observations rotated into either dawn or dusk side depending on Y-position
Values used to create maps	Bin medians, at centroids of bins	
Date generated	1-June-2012	
Creator	John Q. Public	
Additional description and/or comments		

The following is an example of a header file for a numerical model of the magnetosheath:

Parameter	**Value(s)**	**Comments**
Model type	3-D Global MHD	
Name of the model	BATSRUS	
Spatial simulation domain (in R_E)	[-100,-48,-48]- [60, 48, 48]	
Number of grid points used	1, 958, 688	
Average spatial resolution	¼ R_E	
Maximum resolution in key regions	1/16 R_E	domain for high resolution [0,-15,-10]-[10, 15, 10] R_E
Event date and time interval if real event is run	3 July 2012 06:00-08:00 UT	
IMF input vector, (B_x,B_y,B_z) in nT (if fixed input is used)	(0,0,-10)	GSM coordinates
Solar wind density (n_i, in cm^{-3}), velocity (V, in km/s), Temperature (T_i, in K) (if fixed input is used)	10, [-400, 0, 0], 200000	Velocity in aberrated GSE coordinates
Plotted plasma parameters	N_i, V, V_x, V_y, V_z, T_i,β, P_p, S	
Plotted magnetic field parameters	B, P_{mag},B_x, B_y, B_z, J, J_x, J_y, J_z	
Dipole tilt	No dipole tilt	
Conductances (mho)	Pederson: 5.0 Hall: 0.0	
Ring Current Model	Without RCM	
Test particles (if MHD model)	10^6	
Date generated	1-June-2012	
Creator	John Q. Public	
Additional description and/or comments		